NAA-SR-1517

TWO-GROUP CALCULATION OF THE CRITICAL CORE SIZE OF THE SRE REACTOR

ATOMICS INTERNATIONAL
A DIVISION OF NORTH AMERICAN AVIATION, INC.

NAA-SR-1517
COPY_____
43 PAGES
PHYSICS

1

TWO-GROUP CALCULATION OF THE CRITICAL CORE SIZE OF THE SRE REACTOR

PREPARED BY:

F. L. FILLMORE

ATOMICS INTERNATIONAL

A DIVISION OF NORTH AMERICAN AVIATION, INC.
P. O. BOX 309 CANOGA PARK, CALIFORNIA

ISSUE DATE

JULY 1, 1956

CONTRACT AT(04-3)-49

TABLE OF CONTENTS

LIST OF TABLES

LIST OF FIGURES

ABSTRACT

A description is given of the reactor on which the calculations are based. Basic cross sections and other physical data used in the calculation are listed. The required lattice parameters are evaluated, taking into account the details of the lattice cell structure and core structure. Using two-group reflected reactor theory, critical size of the core is calculated for three cases: (1) dry: all materials at 20° C and no sodium in the reactor; (2) wet: sodium present and all materials at 180° C; (3) hot: operating at full power. The flux and adjoint flux is given in both radial and axial directions. Several known perturbations are evaluated for the hot case.

DISTRIBUTION

This report is distributed according to the category "Physics" as given in the "Distribution Lists for Nonclassified Research and Development Reports" TID 4500 (11th Edition), January 15, 1956. A total of 755 copies of this report was printed.

I. DESCRIPTION OF THE REACTOR

The reactor description given here will be sufficient to define the problem being considered, but will not contain irrelevant details. A more complete description is given in Reference 1.

The core and reflector are made up of hexagonal graphite cells each 10 feet high and arranged inside a cylindrical stainless steel tank. Each graphite hexagon is canned in zirconium with 0.035-inch walls. These hexagonal cans are supported by stainless-steel grids at top and bottom. Figure 1 shows a cross section of a typical cell and of the entire assembly and gives the dimensions of the graphite and of the zirconium can. The cell centers form a triangular lattice and their spacing is 11 inches at 20° C. Expansion of the lattice spacing is determined by the temperature of the stainless steel supports.

A circular section is removed from a corner of certain cells so that cylindrical passages are formed running the full length of the cells. These passages, which are also shown in Fig. 1, are incorporated to accommodate thimbles in which control rods, etc., can be placed. There are 17 of these thimbles and they are fairly uniformly distributed throughout the core. Their outer diameter is 2-5/8 inches, and they are wrapped at an 8-inch pitch with 0.0625-inch stainless-steel wire. In this calculation it is assumed that eight of the thimbles are made of stainless steel tubing having 0.035-inch wall and the remainder are made of zirconium tubing having 0.049-inch wall. The interior of all thimbles is assumed to be empty (rods withdrawn) except that the structure of the safety device described in Reference 1 is present in four thimbles. This safety device is assumed to be constructed of zirconium.

The fuel is 2.75 atomic per cent enriched uranium, $N(25)/\left[N(25) + N(28)\right]$, and is located in process tubes which are co-axial with the graphite cells. The loading pattern is shown in Fig. 1. Figure 2 shows a cross section of the fuel-and-process tube. The fuel is in the form of 3/4-inch rods arranged in a seven-rod cluster. Each rod is clad with a 0.011-inch wall stainless-steel tube which is wrapped at a 12-inch pitch with a 0.091-inch stainless-steel wire. There is a 0.009-inch NaK bond between the fuel rod and the cladding. As temperature increases the fuel expands more than the cladding and forces the excess NaK into a reservoir at the top of the fuel rod. The process tube consists of a

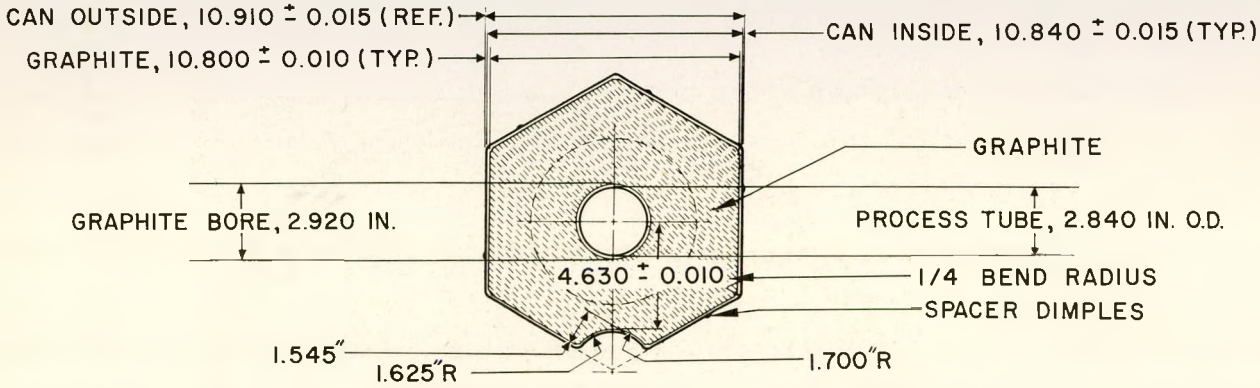

HORIZONTAL CROSS SECTION THROUGH MODERATOR CELL WITH SCALLOPED CORNER WHICH FORMS A PART OF WALL FOR CONTROL AND SAFETY ROD CHANNELS

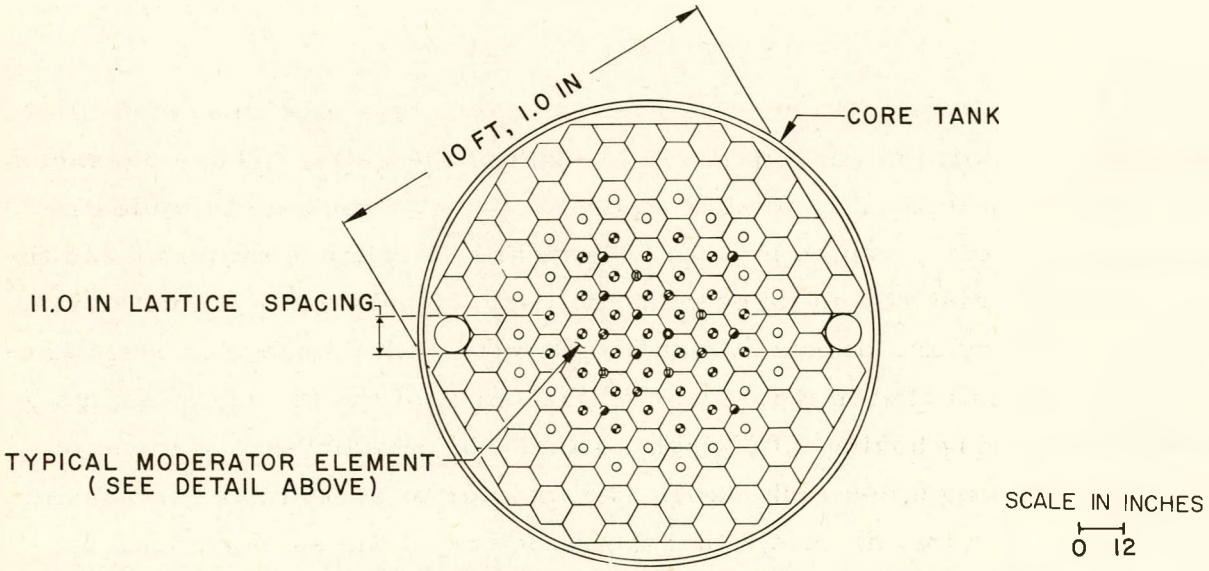

PLAN OF CORE AND REFLECTOR ARRANGEMENT

31	LOADED FUEL CHANNEL
24	EMPTY FUEL CHANNEL FOR INPILE EXPERIMENTS
1	START UP NEUTRON SOURCE
8	CHANNEL AVAILABLE FOR TEMPERATURE MEASUREMENT OR EXPERIMENTAL FACILITIES
4	CONTROL ROD
4	SAFETY ROD

9693-52233

Fig. 1. Arrangement and Detail of Moderator Cells

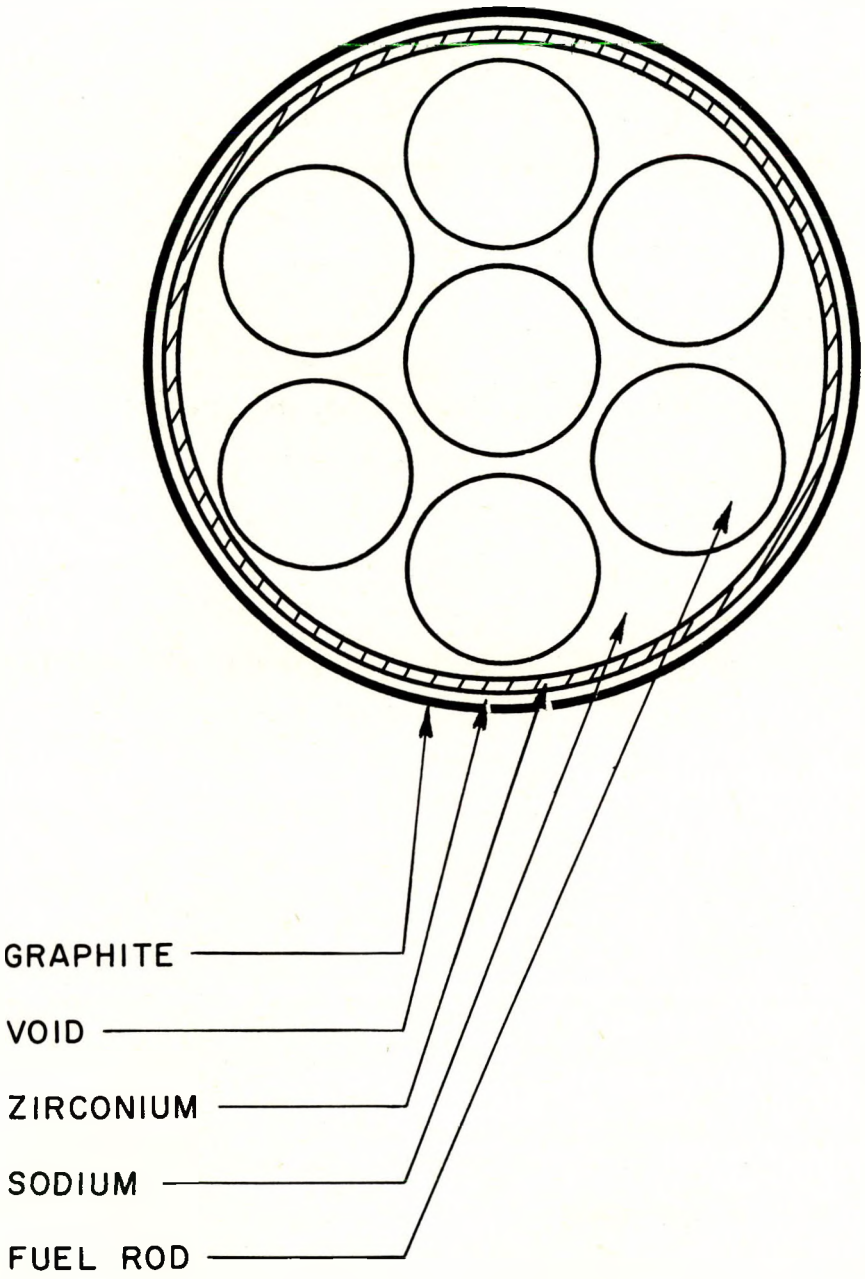

9693-52234

Fig. 2. Cross Section of Fuel Cluster and Process Tube

2.875-inch OD zirconium tube having a 0.035-inch wall. The bore in the graphite is 2.920 inches in diameter.

Sodium coolant flows from bottom to top in the process tube and also between the cell cans. It is assumed that the sodium presses the cell cans in against the graphite, thus eliminating 90 per cent of the void which would otherwise result. The process tube, however, is not distorted by the sodium, so this void remains unaltered. As the temperature rises, the fuel expands more than the process tube, thus reducing the amount of sodium contained therein. On the other hand, the cell spacing expands more than the graphite, so the amount of sodium between the moderator cans increases. The thickness of the sodium layer between zirconium cans when they are pressed flat against the graphite is 0.167 inch at operating temperature.

Average temperatures of the various materials when the reactor is in equilibrium at full power (20 megawatts) were estimated by referring to heat transfer calculations made by members of the engineering staff. The temperature adopted for each material, the density, and the thermal expansion coefficient are given in Table I. The cubical expansion coefficients are given for sodium and NaK liquids.

TABLE I

DENSITIES AND THERMAL EXPANSION COEFFICIENTS

Material	T(°C)	ρ*(gm/cm^3)	Coefficient of Thermal Expansion per° C
Fuel	500	17.865	37×10^{-6}
Graphite	425	1.6344	7.8×10^{-6}
Zirconium	400	6.4583	6.3×10^{-6}
Stainless Steel	410	7.7401	17.3×10^{-6}
Sodium	390	0.85617	2.66×10^{-4}
NaK	420	0.809	2.70×10^{-4}

*The values given in this column retain additional figures in order to provide an accurate comparison of the effects of temperature changes. Using the tabulated expansion coefficients, these densities reduce to handbook values at standard temperatures.

The cross sectional area of the stack (core plus reflector) is 12,060 square inches at 20° C, and its height is 10 feet. In calculating the critical size of the core, the stack will be represented by a right circular cylinder having the above height and cross section. The resulting height and radius are corrected for thermal expansion, and the extrapolation length, $0.71 \lambda_{tr} = 2.13 D_{th}$, is added to each boundary. The resulting dimensions, called R_o and H_o, are used in the criticality calculation. The core height, which equals the length of the uranium fuel, is six feet at 20° C. This is corrected for thermal expansion and the result, called h_c, is used in the criticality calculation. The object of this calculation is to find the core volume required for criticality.

A considerable amount of stainless steel is located above and below the fuel in the process tubes. This was taken into account in calculating the properties of the top and bottom reflectors. Also, although the outermost cell cans in the reflector are made of stainless steel, it is assumed for the sake of simplicity that they are made of zirconium. It is also assumed that all cells not actually loaded with fuel are typical reflector cells. These assumptions greatly simplify the evaluation of the properties of the radial reflector.

The stack dimensions to the extrapolated boundaries, and the core height, are listed in Table II. The condition labeled "hot" refers to the temperatures existing at equilibrium full power operation as shown in Table I.

TABLE II

STACK DIMENSIONS

	Dimensions in cm		
	Dry	Wet	Hot
H_o	308.85	309.25	309.84
R_o	159.27	159.71	160.35
h_c	182.90	183.98	186.15

II. NUCLEAR CROSS SECTIONS AND OTHER DATA

Values for the nuclear cross sections were taken from the AEC compilations[2, 3] and are listed in Table III. Thermal absorption cross sections are Maxwell averages with the graphite temperature characterizing the Maxwellian distribution. The temperature correction for neutron "hardening" was ignored because it is only 10 or 20 degrees centigrade and the moderator temperature is not known this accurately. All thermal absorption cross sections except $\sigma_a(25)$ and $\sigma_f(25)$ were assumed to have 1/v dependence. The capture-to-fission ratio was assumed to be constant at the value $\alpha = 0.184$. Cross sections for stainless steel were averaged for a composition of 67 per cent iron, 20 per cent chromium, 10 per cent nickel, 2 per cent manganese, and 1 per cent silicon. Cross sections for zirconium were averaged for the ingot composition actually being used. The graphite absorption cross section results in a thermal diffusion length of 50 cm for graphite of density 1.60 gms/cm^3 at 20° C. The composition of NaK is 56 per cent sodium and 44 per cent potassium by weight.

The equilibrium xenon and samarium poison cross section is given by[4]

$$\Sigma_a(\text{poison}) = \Sigma_f(25)(1+\delta)(y_{Sm}+Gy_{Xe})$$

where

$$\delta = \frac{(\epsilon-1)\ \nu_{25}}{\nu_{28}-1}$$

y_{Sm} = samarium fission yield = 0.014

y_{Xe} = xenon plus iodine fission yield = 0.059

$$G = \frac{\bar{\phi}}{\bar{\phi}+\lambda_{Xe}/\bar{\sigma}_{(Xe)}} \quad \text{averaged over the core}$$

$\bar{\phi}$ = average flux in the fuel

The average flux in the fuel is given by

$$\phi = \frac{3.12\text{x}10^{10}P}{\bar{\sigma}_f(25)} \frac{238.1+235.1\mathcal{E}}{\mathcal{E}N_o(\rho V)_{fuel}} = 1.33\text{x}10^{13} \text{ neutrons/cm}^2\text{-sec}$$

P = reactor power = 20×10^6 watts for the hot case and zero for the others.

ρV = mass of fuel

N_o = Avogadro's number

$\mathcal{E}$ = N(25)/N(28)

With $\Sigma_f(25) = 0.393\ cm^{-1}$ and G = 0.590, there results:

$$\Sigma_a(\text{poison}) = 0.0210\ cm^{-1}$$

TABLE III

NUCLEAR DATA

Material	σ_a(2200) (barns)	$\bar{\sigma}_s$ (barns)	$\overline{\cos\theta}$	Atomic Weight
Graphite	5.14×10^{-3}	4.8	0.0555	12.00
U^{238}	2.75	8.3	0.0028	238.1
U^{235}	687	10	0.0028	235.1
Sodium	0.50	3.5	0.0290	23.00
Zirconium	0.192	8	0.0073	91.22
Stainless Steel	2.94	9.76	0.0117	55.85
Potassium	1.97	1.5	- -	39.10

For U^{235}

$\bar{\sigma}_f$(20° C) = 504.0 barns f(20° C) = 0.981

$\bar{\sigma}_f$(190° C) = 396.8 barns f(180° C) = 0.980

$\bar{\sigma}_f$(425° C) = 316.0 barns f(425° C) = 1.002

α = 0.184

ν = 2.46

$\mathcal{E} = N_{25}/N_{28}$ = 0.02829

Poisons

$\bar{\sigma}_a$(Xe-135) = 2.14×10^6 barns at 425° C

λ(Xe) = $2.09 \times 10^{-5}\ sec^{-1}$

Total xenon fission yield = 0.059

Samarium fission yield = 0.014

TABLE III (continued)

Resonance Data[4, 5]

$$\left(\int_{E_2}^{E_1} \sigma_{res}\,\frac{dE}{E}\right)_{eff} = 7.6\left[\frac{1}{F}+3.40\frac{S}{M}\right] \text{ barns with the 1/v tail subtracted.}$$

$$\mathscr{K}_u = 0.420 \text{ cm}^{-1} \text{ for natural uranium at 20° C}$$

$$\frac{d\mathscr{K}_u}{d\mathcal{E}} = 2.46 \text{ cm}^{-1}$$

$$\sigma_s(\text{fuel}) = 8.2 \text{ barns}$$
$$\sigma_s(\text{graphite}) = 4.7 \text{ barns}$$
$$\xi(\text{graphite}) = 0.1577$$
$$\ell n\ E_1/E_2 = 2.6$$
$$\mathscr{K}_m = 0.162 \text{ cm}^{-1} \text{ for graphite of density } 1.65 \text{ gm/cm}^3$$

Uranium cross sections averaged over the fission spectrum (barns)

$\sigma_t(28) = 7.10$	$\sigma_t(25) = 7.1$
$\sigma_f(28) = 0.28$	$\sigma_f(25) = 1.2$
$\sigma_{in}(28) = 1.85$	$\sigma_{in}(25) = 1.5$
$\sigma_c(28) = 0.09$	$\sigma_c(25) = 0.2$
$\nu_{28} = 2.5$	$\nu_{25} = 3.0$

Average scattering cross sections for fast neutrons

$\bar{\sigma}_s$(uranium)	= 7.4 barns
$\bar{\sigma}_s$(graphite)	= 4.40 barns
$\bar{\sigma}_s$(sodium)	= 3.7 barns
$\bar{\sigma}_s$(stainless steel)	= 7.7 barns
$\bar{\sigma}_s$(zirconium)	= 8.6 barns
$\bar{\Sigma}_s$(NaK)	= 0.050 cm^{-1}

III. CELL MODEL AND THERMAL FLUX IN A LATTICE CELL

For the calculation of the thermal utilization and thermal diffusion length it is necessary to flux-weight the absorption and transport cross sections over the lattice cell. We require the volume fractions of the materials which constitute the cell and the average thermal flux in each material. The flux can be obtained experimentally with good accuracy, since only relative values are needed. As these measurements have not yet been made for the SRE lattice cell, a calculation is necessary. While methods exist for the accurate calculation of the flux, they involve considerable computational labor and are complicated by the structure of the SRE fuel clusters. In order to avoid these complications, a simpler method was used which applied elementary one-group diffusion theory to the five-region model of the lattice cell shown in Fig. 3. It is well known that elementary diffusion theory gives inaccurate results in such calculations, but flux measurements were available for a seven-rod fuel cluster which had somewhat different dimensions and enrichment and which was immersed in D_2O moderator, so it was possible to estimate the corrections to apply to the calculated results. It is believed that the uncertainty introduced into the thermal utilization because of the lack of accurate knowledge about the flux is less than 1/2 per cent.

The cell model used to calculate the flux will now be described. The regions in Fig. 3 are numbered 1 to 5, starting with the innermost. The boundaries of these regions are determined as follows: r_1 = radius of a fuel rod without its cladding and bond, r_2 and r_3 are determined by requiring that the area of the annulus which they bound shall equal the area of six fuel rods and that the average of r_2 and r_3 shall equal the radius of the circle upon which the centers of the six outer fuel rods are located, r_4 is the radius of the graphite bore, and r_5 is the radius of a circle whose area equals that of the hexagonal cell. Values of these radii are given in Table IV.

It was assumed that Regions 1 and 3 consisted only of fuel, Region 5 only of graphite, Region 2 of a homogeneous mixture in the proper ratios of sodium and stainless steel, and Region 4 of a homogeneous mixture of sodium, stainless steel, and zirconium. If the sodium is removed from the cell, as in the dry case, it is assumed that the flux is constant in Regions 2 and 4. The calculation is then carried out in the same manner as in the other cases. Average thermal absorption and transport cross sections for each region were calculated for each of the

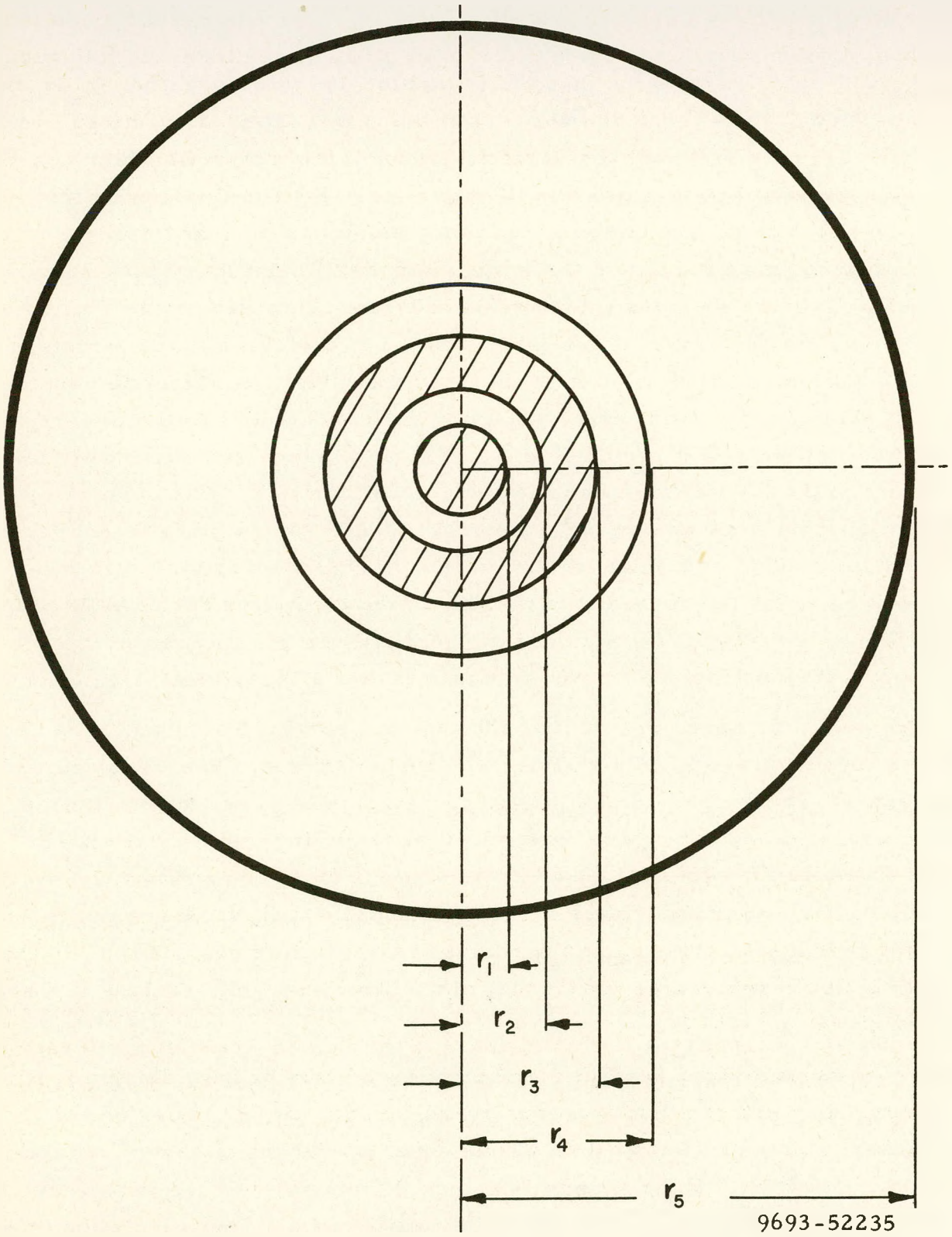

Fig. 3. Model Used to Represent the Seven Rod Fuel Cluster and the Hexagonal Lattice Cell

3 cases being considered and are listed in Table IV. The inverse diffusion length and diffusion coefficient for each region was then calculated from the following formulas:

$$\frac{\mathscr{K}}{\Sigma_s + \Sigma_a} = \tanh \frac{\mathscr{K}}{\Sigma_s} \quad \text{(Regions 1 and 3)}$$

$$\mathscr{K}^2 = 3\Sigma_{tr}\Sigma_a \left[1 - \frac{4}{5} \frac{\Sigma_a}{\Sigma_s + \Sigma_a}\right] \quad \text{(Regions 2, 4, and 5)}$$

$$D = \Sigma_a / \mathscr{K}^2$$

$$\Sigma_{tr} = \Sigma_s(1-\bar{\mu}) + \Sigma_a$$

Absorption cross sections for the hot case (operation at full power) include equilibrium xenon and samarium poison.

The desired solution of the one-group diffusion equation for an infinitely long cylinder is of the form

$$\phi_i(r) = A_i I_o(\mathscr{K}_i r) + B_i K_o(\mathscr{K}_i r) + \frac{Q_i}{\mathscr{K}_i^2 D_i}; \qquad r_{i-1} \le r \le r_i$$

where $i = 1, 2, 3, 4, 5$ refers to regions shown in Fig. 3.

$\mathscr{K}_i$ = inverse diffusion length in the i-th region.

D_i = diffusion coefficient in the i-th region.

Q_i = source in the i-th region, which we take to be zero in Regions 1 to 4 and constant in Region 5.

I_o and K_o are Bessel functions: A_i and B_i are constants which are determined by the boundary conditions. The condition that the flux be finite at $r = 0$ requires that $B_1 = 0$, and we may normalize by taking $A_1 = 1$. Symmetry demands the vanishing of the neutron current at $r = r_5$, which requires that

$$B_5 = A_5 \frac{I_1(\mathscr{K}_5 r_5)}{K_1(\mathscr{K}_5 r_5)}$$

TABLE IV 16

DIMENSIONS AND NUCLEAR DATA FOR THE CELL MODEL

Region	r_i(cm)			Σ_a(cm^{-1})			$\bar{\mu}$	Σ_{tr}(cm^{-1})			$\mathcal{K}$(cm^{-1})		
	dry	wet	hot	dry	wet	hot		dry	wet	hot	dry	wet	hot
1	0.9520	0.9577	0.9689	0.8975	0.6960	0.5560	0.0028	1.2951	1.0865	0.9325	1.292	1.079	0.8969
2	1.671	1.662	1.649	- -	0.03431	0.02763	0.0290	- -	0.2281	0.2221	- -	0.1419	0.1269
3	2.869	2.875	2.890	0.8975	0.6960	0.5560	0.0028	1.2951	1.0865	0.9325	1.292	1.079	0.8969
4	3.708	3.712	3.719	- -	0.01480	0.01480	0.0290	- -	0.1577	0.1548	- -	0.07930	0.07103
5	14.670	14.710	14.764	3.775×10^{-4}	3.02×10^{-4}	2.23×10^{-4}	0.0555	0.3759	0.3745	0.3723	0.02063	0.01844	0.01645

The continuity of flux and current at the interfaces leads to the following equations for the remaining constants

$$\begin{pmatrix} A_{i+1} \\ \\ B_{i+1} \end{pmatrix} = \varkappa_{i+1} r_i \begin{pmatrix} K_1 & K_o \\ \varkappa_{i+1} r_i & \\ I_1 & -I_o \end{pmatrix} \begin{pmatrix} 1 & 0 \\ 0 & \frac{D_i \varkappa_i}{D_{i+1} \varkappa_{i+1}} \end{pmatrix} \begin{pmatrix} I_o & K_o \\ \varkappa_i r_i & \\ I_1 & -K_1 \end{pmatrix} \begin{pmatrix} A_i \\ \\ B_i \end{pmatrix}$$

where i = 1, 2, 3.

$$\begin{pmatrix} A_5 \\ \\ \frac{Q_5}{\varkappa_5 D_5} \end{pmatrix} = \frac{1}{Y_{4,5}} \begin{pmatrix} 0 & -1 \\ Y_{4,5} & -W_{4,5} \end{pmatrix} \begin{pmatrix} 1 & 0 \\ 0 & \frac{D_4 \varkappa_4}{D_5 \varkappa_5} \end{pmatrix} \begin{pmatrix} I_o & K_o \\ \varkappa_4 r_4 & \\ I_1 & -K_1 \end{pmatrix} \begin{pmatrix} A_4 \\ \\ B_4 \end{pmatrix}$$

The expression $\varkappa r$ in the center of a matrix is the argument of each Bessel function in that matrix. The W's and Y's are defined by

$$W_{4,5} = \begin{vmatrix} I_o(\varkappa_5 r_4) & K_o(\varkappa_5 r_4) \\ I_1(\varkappa_5 r_5) & -K_1(\varkappa_5 r_5) \end{vmatrix}$$

$$Y_{4,5} = \begin{vmatrix} I_1(\varkappa_5 r_4) & -K_1(\varkappa_5 r_4) \\ I_1(\varkappa_5 r_5) & -K_1(\varkappa_5 r_5) \end{vmatrix}$$

The average flux in the i-th region is given by

$$\bar{\phi}_i = \frac{2\pi\psi_i}{V_i}$$

where V_i is the volume of the i-th region, and

$$\psi_i = \frac{A_i}{\mathcal{K}_i}\left[rI_1(\mathcal{K}_i r)\right]_{r_{i-1}}^{r_i} - \frac{B_i}{\mathcal{K}_i}\left[rK_1(\mathcal{K}_i r)\right]_{r_{i-1}}^{r_i} + \frac{Q_i}{2\mathcal{K}_i^2 D_i}\left[r_i^2 - r_{i-1}^2\right]$$

Figure 4 shows a graph of the flux in a cell as calculated by the above method. Table V gives the computed values of $\bar{\phi}_i$ and $\bar{\phi}(r_i)$ together with their "corrected" values, which were obtained by applying corrections which were indicated by the flux measurements made in the seven-rod fuel cluster previously mentioned to the computed values. A disadvantage factor of 0.945 was estimated for the stainless steel thimbles by means of a control rod type of flux calculation.

The volume fractions of each material in the cell were calculated. There are 17 thimbles in the core. The materials in the thimbles were included in this calculation by assigning 17/31 of the total material in the thimbles to a cell. Table VI gives the results of this calculation for the 3 cases being considered. Note that the volume fraction of several of the materials is divided into more than one part. This is done because of the flux variation in the cell.

TABLE V

AVERAGE FLUX IN CELL

	Calculated Flux			Adjustment	Adjusted Flux		
	dry	wet	hot	Factor	dry	wet	hot
$\bar{\phi}_1$	1.2015	1.1395	1.0974	1.00	1.2015	1.1395	1.0974
$\phi(r_1)$	1.4155	1.2853	1.1979	1.03	1.4580	1.3239	1.2338
$\bar{\phi}_2$	1.4155	1.3533	1.2382	1.03	1.4580	1.3939	1.2754
$\phi(r_2)$	1.4155	1.4085	1.2905	1.03	1.4580	1.4508	1.3293
$\bar{\phi}_3$	2.2972	2.0946	1.7389	1.04	2.4931	2.1784	1.8084
$\phi(r_3)$	3.8558	3.0605	2.3438	1.07	4.1257	3.2747	2.5078
$\bar{\phi}_4$	3.8558	3.3094	2.5006	1.20	4.6269	3.9713	3.0007
$\phi(r_4)$	3.8558	3.5469	2.6721	1.30	5.0125	4.6110	3.4737
$\bar{\phi}_5$	9.5165	7.0352	5.2859	1.20	11.4198	8.4422	6.3431
$\phi(r_5)$	10.7420	8.4906	6.2080	1.20	12.8904	10.1887	7.4495

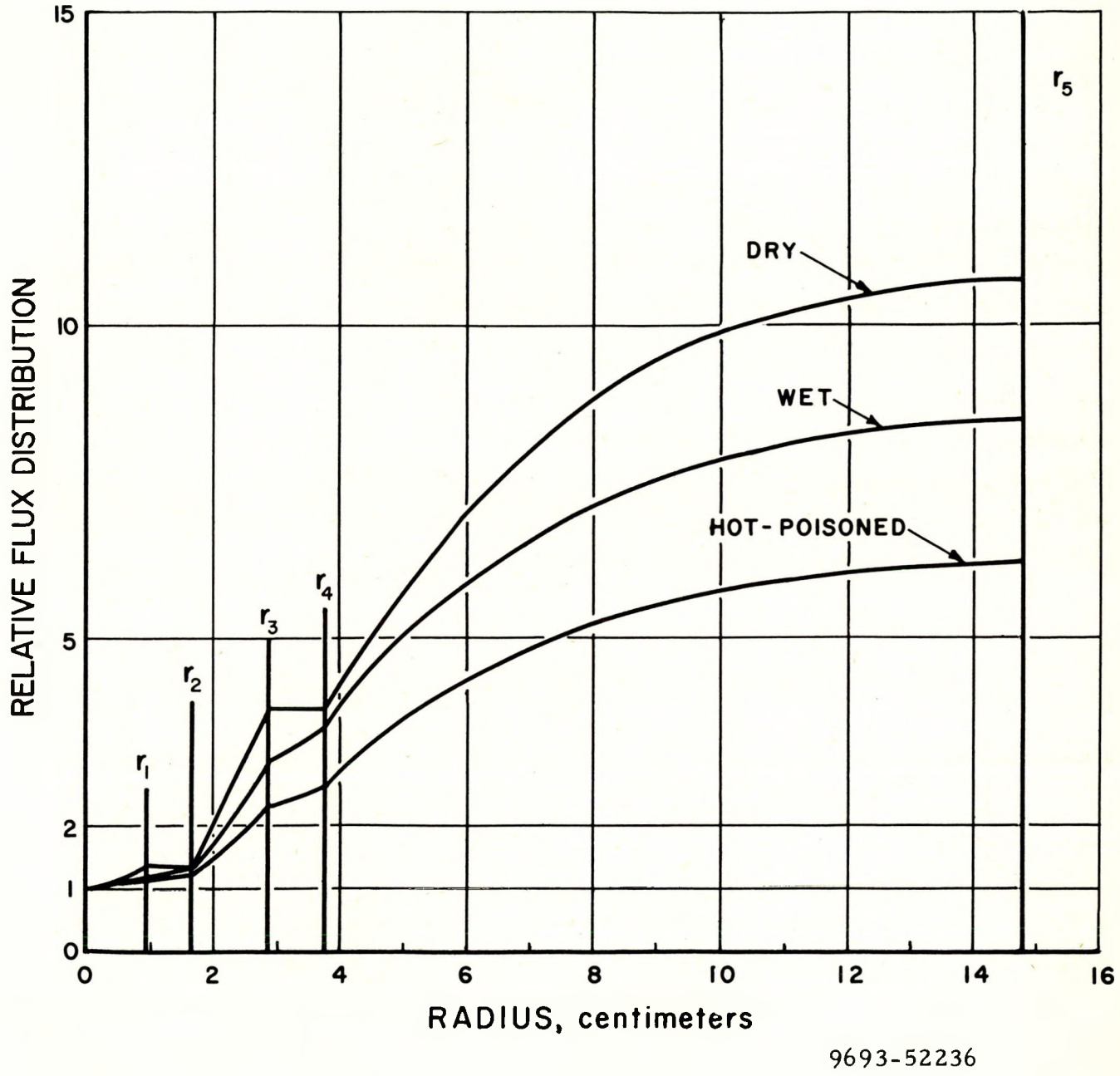

Fig. 4. Flux in Lattice Cell Model

TABLE VI

VOLUME FRACTIONS FOR EACH MATERIAL IN A CELL

Material	Dry	Wet	Hot
Fuel			
1 rod	0.004211	0.004239	0.004307
6 rods	0.025268	0.025432	0.025840
Stainless Steel			
Cladding 1 rod	0.000322	0.000322	0.000322
Cladding 6 rods	0.001930	0.001930	0.001930
8 thimbles	0.000709	0.00709	0.000709
NaK Bond			
1 rod	0.000216	0.000188	0.000116
6 rods	0.001298	0.001126	0.000698
Zirconium			
Process tube	0.002980	0.002969	0.002955
Moderator can and 9 thimbles	0.914388	0.014338	0.014269
Sodium			
Region 2	0.006502	0.006460	0.006415
Region 4	0.019105	0.018983	0.018849
Between moderator cans and in 17 thimble channels	0.034486	0.037247	0.040855
Void			
At process tube wall	0.002056	0.002029	0.002020
In 17 thimbles and between moderator and can	0.025083	0.024987	0.024917
Graphite	0.861446	0.859041	0.855798

IV. RECIPES FOR CALCULATING THE LATTICE CONSTANTS

The formulas given in this section are consistent (although not always identical) with those of Reference 4. The symbols employed have their usual meaning unless otherwise defined.

A. CROSS SECTIONS

The flux-averaged absorption and transport cross sections over the cell are given by

$$\bar{\Sigma} = \frac{\sum_i \bar{\phi}_i V_i \Sigma_i}{\sum_i \bar{\phi}_i V_i}$$

where V_i represents the volume fractions and the summation is over all materials in the cell including the void.

B. THERMAL UTILIZATION

$$f = \frac{(\phi_1 V_1 + \phi_3 V_3)\, \Sigma_a(\text{fuel})}{\sum_i \phi_1 V_1 \Sigma_{ai}}$$

C. THERMAL DIFFUSION LENGTH

$$L^2 = \frac{1}{3 \bar{\Sigma}_a \bar{\Sigma}_{tr}}$$

D. RESONANCE ESCAPE

$$p = e^{-1/T}$$

where

$$T = \frac{\text{neutrons removed from the resonance energy by slowing down in the moderator}}{\text{resonance neutrons absorbed in the fuel}}$$

The usual formula for T is written as

$$T = \frac{V_m \xi \Sigma_s(\text{mod})}{V_u N_u \left(\int \sigma_{res} \frac{dE}{E} \right)_{eff}} + (E-1)$$

where the subscript m refers to graphite and u refers to fuel. (E-1) is the well known excess "absorption" term, where "absorption" means removal of neutrons from the resonance energy region by the process of slowing down, and is calculated only for Region 5 of the cell model shown in Fig. 3. The inverse diffusion length for resonance neutrons in the graphite is required for its evaluation and is given by

$$\varkappa_m^2 = 3\Sigma_{tr}\Sigma_{s1}\left[1-\frac{4}{5}\frac{\Sigma_{s1}}{\Sigma_s+\Sigma_{s1}}\right]$$

where the slowing down cross section Σ_{s1} is defined by

$$\Sigma_{s1} = \frac{\xi\Sigma_s}{\ln E_1/E_2}$$

It was estimated[5] that the logarithmic energy band for resonance neutrons when the 1/v tail is deleted from the U^{238} effective resonance absorption integral is $\ln E_1/E_2 = 2.6$. We are aware of the value 5.6 which is given in the reactor handbook but have not been able to justify the use of this value.

The value used for the effective resonance integral in U^{238} with the 1/v absorption removed is

$$\left(\int\sigma_{res}\frac{dE}{E}\right)_{eff} = 7.6\left[\frac{1}{F}+3.40\frac{S}{M}\right] \text{ barns.}$$

F is the disadvantage factor of the 7 fuel rods for resonance neutrons which was taken to be

$$F = \frac{\varkappa_u r_1\sqrt{7}}{2}\;\frac{I_o(\varkappa_u r_1\sqrt{7})}{I_1(\varkappa_u r_1\sqrt{7})}$$

The value of $\varkappa_u$ was adjusted for changes in temperature and enrichment. The data used are given in Table III.

The S/M term in the effective resonance integral was calculated as suggested by Dr. E. R. Cohen by taking the surface to be that given by placing a taut rubber band around the outside of the fuel rods. This is the proper

surface to use provided that a neutron which enters the region inside this surface cannot escape without traversing a fuel rod, which is the case for the 7 rod fuel clusters if scattering in the sodium is neglected.

Correction to p for the doppler broadening of the resonances due to a temperature increase of θ ° C was taken to be

$$p(\theta) = p_o \exp\left[-\frac{1.0\times10^{-4}\theta}{T}\left(1-\frac{E-1}{T}\right)\right]$$

The value of the temperature coefficient of the effective resonance integral was taken to be 1.0×10^{-4} per degree centigrade.[6]

E. ETA

$$\eta = \frac{\nu\bar{\sigma}_f(25)}{\bar{\sigma}_a(25)+\frac{1}{\mathcal{E}}\bar{\sigma}_a(28)+\frac{\Sigma_a\,(\text{poison})}{N_{25}}}$$

F. EPSILON

$$\epsilon = 1 + \frac{\left[(\nu-1)\,\sigma_f - \sigma_c\right]P}{\sigma_t - \left[\nu\sigma_f + \sigma\right]P}$$

where the cross sections are averaged over the fission spectrum and

$$\sigma_t = \sigma_c + \sigma_f + \sigma_{in} + \sigma_e$$

These cross sections are for the enriched fuel and are given by

$$\sigma_{fuel} = \frac{\mathcal{E}}{1+\mathcal{E}}\,\sigma_{25} + \frac{1}{1+\mathcal{E}}\,\sigma_{28}$$

P is the first collision probability for a fission neutron in the fuel cluster and is obtained from curves of Reference 7 which gives P for hollow cylinders. The hollow cylinder used here is Region 3 of Fig. 3. with the inner fuel rod distributed uniformly on the inside of this region. The variation of ϵ with temperature is negligible and was not investigated.

G. AGE

$$\tau = \left[\tau_f - (\tau_f - \tau_{in}) \frac{\sigma_{in}}{\sigma_{tot}} P + \frac{D}{\xi \Sigma_s} \ln \frac{1.44}{16kT}\right] \left(\frac{\rho_o}{\rho}\right)^2 \frac{1}{V_m (1 - V_o)}$$

τ_f = age in graphite of fission neutrons to the indium resonance

τ_{in} = age in graphite of inelastically scattered fission neutrons to the indium resonance

P = collision probability for fission neutrons in the fuel cluster

ρ = graphite density

V_o = volume fraction of the void

$V_m = \sum_i V_i \frac{(\xi \Sigma_s)_i}{(\xi \Sigma_s)_{graphite}}$, where the summation is over all the cell

$\frac{D}{\xi \Sigma_s}$ = 15.01 for epithermal neutrons in graphite of density 1.60 gm/cm^3

The correction of the age from the indium resonance to thermal energy is made to the energy 16kT.[8]

H. FAST NEUTRON-TRANSPORT CROSS SECTION

Absorption is negligible and it was assumed that the average fast neutron flux was constant over the cell so that no flux weighting of the cross sections is required.

$$\bar{\Sigma}_{tr} = \bar{\Sigma}_i V_i (1 - \bar{\mu}_i) \Sigma_{si}$$

where $\bar{\mu}$ is the average cosine of the scattering angle in the laboratory system. The values used for the average scattering cross section for fast neutrons are listed in Table III. The temperature dependence of $\bar{\Sigma}_{tr}$ was assumed to be the same as for graphite, namely $(1 - 3\alpha_{gr}\Delta T)$.

The diffusion coefficient for fast neutrons is

$$D = \frac{1}{3\Sigma_{tr}}$$

The slowing down cross section for the cell is

$$\Sigma_{sl} = \frac{D}{\tau}$$

V. SUMMARY OF CALCULATED RESULTS FOR THE LATTICE

The results of the lattice calculations which were outlined in the preceeding section are given in Table VII. The buckling listed is calculated from the formula

$$1+L^2B^2 = k_\infty e^{-\tau B^2}$$

TABLE VII

CORE DATA

	Dry	Wet	Hot
η	1.815	1.810	1.741
ϵ	1.0433	1.0430	1.0423
p	0.8565	0.8560	0.8526
f	0.8784	0.8204	0.8384
k_∞	1.4222	1.3257	1.2971
$\Sigma_a(cm^{-1})$	0.006321	0.006231	0.005553
$L^2(cm^2)$	149.85	152.05	172.38
$D_{th}(cm)$	0.9472	0.9474	0.9572
$\tau(cm^2)$	379.5	349.1	346.8
$D_f(cm)$	1.0582	1.0469	1.0572
$B^2(cm^{-2})$	675×10^{-6}	566×10^{-2}	505×10^{-6}

VI. REFLECTOR

The radial and axial reflectors must be treated separately because of the different geometries and materials involved. The radial reflector was assumed to consist of solid graphite hexagons, whose dimensions are identical with those used in the core, canned in zirconium cans identical with the core cans. No flux weighting of cross sections is required because there is no strongly absorbing material contained in the cell. Volume fractions for the three cases under study are given in Table VIII. Calculation of Σ_a, L^2, τ, and D_f then proceed according to the same plan as used in the core, and the results are also shown in Table VIII.

TABLE VIII

RADIAL REFLECTOR DATA

Material	Volume Fraction		
	Dry	Wet	Hot
Graphite	0.963967	0.961040	0.957644
Zirconium	0.012582	0.012527	0.012452
Sodium	0.00000	0.025756	0.029338
Void	0.023451	0.000677	0.000566
	Results		
$\bar{\Sigma}_a(cm^{-1})$	0.000455	0.000582	0.000480
$L^2(cm^2)$	2000.0	1562.5	1923.1
$\tau(cm^2)$	318.26	307.03	304.91
$D_f(cm)$	0.9906	0.9908	0.9996

It is difficult to evaluate the properties of the axial reflector because of its more complicated geometry and the lack of symmetry between the top and bottom reflectors. What is desired is an average homogeneous reflector which has the same effect on reactivity as have the top and bottom reflectors combined. This will be achieved here by simply flux weighting the several materials present in the reflector. The careful calculation of volume fractions and disadvantage

factors and the evaluation of streaming in the sodium-filled process tubes involves more labor than is justified. The results which follow were obtained by making several simplifying approximations.

The graphite, zirconium, and void-volume fractions are the same as those obtained for the core, because each cell is simply a extension in the vertical direction of a core cell. The effect of the zirconium and void at the top and bottom of the hexagons was neglected because this is a low flux region. The volume of the stainless steel hangar rods and the irregularly shaped end caps on the fuel cluster was estimated and added to that in the thimbles. Sodium makes up the remainder of the cell volume. A disadvantage factor for the process tube was estimated by means of a control rod type flux calculation for the hangar rod. It was found that the flux was depressed about 10 per cent in the process tube.

The volume fractions and relative flux in the various materials are given in Table IX. The calculated values of $\overline{\Sigma}_a$, L^2, and D_f are also shown.

TABLE IX

AXIAL REFLECTOR DATA

Material	Volume Fraction			$\overline{\phi}$
	Dry	Wet	Hot	
Graphite	0.86145	0.85904	0.85580	1.00
Steel in process tube	0.00284	0.00284	0.00284	0.90
Sodium in process tube	0.00000	0.05584	0.05564	0.90
Zirconium in process tube	0.00298	0.00297	0.00295	0.90
Void in process tube	0.05807	0.00203	0.00202	0.90
Steel in Thimbles	0.00071	0.00071	0.00071	0.945
Zirconium in can	0.01439	0.01434	0.01427	1.00
Void at cell boundary	0.05956	0.02499	0.02492	1.00
Sodium at cell boundary	0.00000	0.03725	0.04086	1.00

Results

	Dry	Wet	Hot
$\Sigma_a(cm^{-1})$	0.001183	0.001689	0.001335
$L^2(cm^2)$	840.34	579.04	740.74
$\tau(cm^2)$	393.13	348.19	345.86
$D_f(cm)$	1.0920	1.0710	1.0818

VII. THE TWO-GROUP PROBLEM, CRITICAL SIZE, AND FLUX

In attempting to solve the two-group, two-region boundary value problem using the method of separation of variables in cylindrical coordinates for a reactor reflected axially as well as radially, one finds that the boundary conditions at the core-reflector boundary are not satisfied by the fundamental mode solution. Therefore, this well-known method fails in this case. However, an approximate solution can be obtained by treating the radial problem as a cylindrical reactor which is reflected radially but is bare on the ends, and the axial problem as a cylindrical reactor which is reflected on the ends but is bare radially. The material buckling is found by solving the characteristic equation,

$$(1+L^2B^2)\,(1+\tau B^2) = k_\infty$$

The buckling is then divided into radial and axial components

$$B^2 = B_r^2+B_z^2$$

It is desired to find the core volume which will make the reactor critical. Since the height of the core and the height and radius of the stack are given, the parameters to be adjusted to produce criticality are the axial buckling and the core radius. The axial problem is solved first by assuming a value for B_z^2 and finding the core height h which produces criticality. If this calculated value of h is not equal to the actual core height, another value of B_z^2 is tried and the calculation repeated. This procedure can be continued until the calculated value of h is equal to the actual core height. The radial problem is then solved for the critical radius of the core R_c, using the axial buckling which gave the correct core height.

It is actually not necessary to continue the solution of the axial problem until h is exactly equal to the core height, because if h is close to the actual height, the critical volume of the core will be given to sufficient accuracy by $\pi R_c^2 h$. Since the volume of a cell is known, the number of cells which must be loaded can then be found. The thermal and fast fluxes and the adjoint functions are next evaluated, and if h is within one or two centimeters of the actual height, they will be given with sufficient accuracy for use in perturbation theory calculations.

The equations used in solving the two-group, two-region problems are given below. Subscripts 1 and 2 refer to fast and thermal neutrons respectively: subscripts c and o refer to core and reflector respectively. μ^2 and $-\nu^2$ are the two roots of the characteristic equation.

Axial flux

$$\phi_{1c} = A \cos B_z z + C \cosh \gamma z \qquad 0 \le |z| \le h/2$$

$$\phi_{2c} = AS_c \cos B_z z + CT_c \cosh \gamma z$$

$$\phi_{10} = F \sinh \mathcal{K}_{10}\left(\frac{Ho}{2} - z\right)$$

$$\phi_{20} = FS_o \sinh \mathcal{K}_{10}\left(\frac{Ho}{2} - z\right) + G \sinh \mathcal{K}_{20}\left(\frac{Ho}{2} - z\right) \qquad h/2 \le |z| \le \frac{Ho}{2}$$

$$\gamma^2 = \mu^2 + \nu^2 - B_z^2$$

$$\mathcal{K}_{10}^2 = \frac{1}{\tau_o} + B_r^2$$

$$\mathcal{K}_{20}^2 = \frac{1}{L_o^2} + B_r^2$$

$$T_c = \frac{p_c D_{1c}}{\tau_c D_{2c}} \quad \frac{1}{1/L_c^2 + \mu^2}$$

$$T_c = \frac{p_c D_{1c}}{\tau_c D_{2c}} \quad \frac{1}{1/L_c^2 - \nu^2}$$

$$S_o = \frac{p_o D_{10}}{\tau_o D_{20}} \quad \frac{1}{\mathcal{K}_{20}^2 - \mathcal{K}_{10}^2}$$

The criticality equation is

$$\begin{vmatrix} \cos B_z h/2 & \cosh\gamma h/2 & -\sinh \mathcal{K}_{10}\frac{H_o - h}{2} & 0 \\ -D_{1c} B_z \sin B_z h/2 & D_{1c}\gamma \sinh\gamma h/2 & D_{10}\mathcal{K}_{10}\cosh \mathcal{K}_{10}\frac{H_o - h}{2} & 0 \\ S_c \cos B_z h/2 & T_c \cosh\gamma h/2 & -S_o \sinh \mathcal{K}_{10}\frac{H_o - h}{2} & -\sinh \mathcal{K}_{20}\frac{H_o - h}{2} \\ -D_{2c} S_c B_z \sin B_z h/2 & D_{2c} T_c \gamma \sinh\gamma h/2 & D_{20} S_o \mathcal{K}_{10} \cosh \mathcal{K}_{10}\frac{H_o - h}{2} & D_{20}\mathcal{K}_{20} \cosh \mathcal{K}_{20}\frac{H_o - h}{2} \end{vmatrix} = 0$$

Axial adjoint functions

$$\phi^*_{1c} = A^*\cos B_z z + C^*\cosh\gamma z \qquad 0 \le z \le h/2$$

$$\phi^*_{2c} = A^*S^*_c\cos B_z z + C^*T^*_c\cosh\gamma z$$

$$\phi^*_{10} = G^*T^*\sinh\mathcal{K}_{20}\left(\frac{H_o}{2} - z\right) + F^*\sinh\mathcal{K}_{10}\left(\frac{H_o}{2} - z\right) \qquad h/2 \le z \le H_o/2$$

$$\phi^*_{20} = G^*\sinh\mathcal{K}_{20}\left(\frac{H_o}{2} - z\right)$$

$$S^*_c = \frac{1+\tau_c\mu^2}{p_c}$$

$$T^*_c = \frac{1-\tau_c\nu^2}{p_c}$$

$$T^*_o = \frac{p_c}{\tau_o(\mathcal{K}^2_{10}-\mathcal{K}_{20})}$$

Radial flux

$$\phi_{1c} = \bar{A}J_o(\alpha r)+\bar{C}I_o(\beta r) \qquad 0\le r\le R_c$$

$$\phi_{2c} = \bar{A}S_cJ_o(\alpha r)+\bar{C}T_cI_o(\beta r)$$

$$\phi_{10} = \bar{F}Z(\mathcal{K}_{10}, r) \qquad R_c \le r \le R_o$$

$$\phi_{20} = \bar{F}S_oZ(\mathcal{K}_{10}, r)+\bar{G}Z(\mathcal{K}_{20}, r)$$

$$\alpha^2 = \mu^2 - B_z^2$$

$$\beta^2 = \nu^2 + B_z^2$$

$$Z(\mathcal{H}, r) = I_o(\mathcal{H} r) - \frac{I_o(\mathcal{H} R_o)}{K_o(\mathcal{H} R_o)} K_o(\mathcal{H} r)$$

$$\mathcal{H}_{10}^2 = \frac{1}{\tau_o} + B_z^2$$

$$\mathcal{H}_{20}^2 = \frac{1}{L_o^2} + B_z^2$$

The criticality equation is

$$\begin{vmatrix} J_o(\alpha R) & I_o(\beta R) & -Z(\mathcal{H}_{10}, R) & 0 \\ -D_{1c}\alpha J_1(\alpha R) & D_{1c}\beta I_1(\beta R) & -D_{10} Z'(\mathcal{H}_{10}, R) & 0 \\ S_c J_o(\alpha R) & T_c I_o(\beta R) & -S_o Z(\mathcal{H}_{10}, R) & -Z(\mathcal{H}_{20}, R) \\ -D_{2c} S_c \alpha J_1(\alpha R) & D_{2c} T_c \beta I_1(\beta R) & -D_{20} S_o Z'(\mathcal{H}_{10}, R) & -D_{20} Z'(\mathcal{H}_{20}, R) \end{vmatrix} = 0$$

Radial adjoint functions

$$\phi_{1c}^* = \bar{A}^* J_o(\alpha r) + \bar{C}^* I_o(\beta r)$$

$$\phi_{2c}^* = \bar{A}^* S_c^* J_o(\alpha r) + \bar{C}^* T_c^* I_o(\beta r) \qquad o \le r \le R_c$$

$$\phi_{10}^* = \bar{G}^* T_o^* Z(\mathcal{H}_{20}, r) + \bar{F}^* Z(\mathcal{H}_{10}, r)$$

$$\phi_{20}^* = \bar{G}^* Z(\mathcal{H}_{20}, r) \qquad R_c \le r \le R_o$$

In calculating the axial and radial problems it must be remembered that the properties of the outer region have different values in each case. Although the formula for S_o and T_o^* are the same in both cases, their numerical values are not.

The critical volume was calculated for each of the three cases being considered and the number of cells required to give this volume was then determined. The results are as follows:

dry	$V = 1.73 \times 10^6 cm^3$	N = 13.81
wet	$V = 2.936 \times 10^6 cm^3$	N = 23.48
hot, poisoned	$V = 3.572 \times 10^6 cm^3$	N = 28.03

The flux and adjoint functions were calculated for each case and normalized to unit fast flux at the center of the reactor. Figures 5, 6, and 7 show the axial flux and adjoint; Fig. 8, 9, and 10 show the radial flux and adjoint.

The average value of the thermal flux over the core was calculated by normalizing both radial and axial thermal flux to unity at the center of the core and then evaluating the expression

$$\bar{\phi} = \frac{1}{\pi R_c^2 h} \int_{\text{core}} \phi_{2c}(r)\phi_{2c}(Z) 2\pi r \, dr \, dz$$

The result for the hot case is

$$\phi = 0.647$$

The ratio of the peak-to-average flux along the z-axis is 1.236.

VIII. GENERATION TIME AND PERTURBATIONS FOR THE HOT-POISONED CASE

The designed reactor differs somewhat from the reactor described in Section I of this report, so it is necessary to investigate the effect of the known differences on the criticality calculations. This was done by means of perturbation theory. The basis for these calculations is the reactivity formula

$$\rho = \omega \ell + \omega \sum_{i=1}^{6} \frac{\beta_i}{\lambda_i + \omega}$$

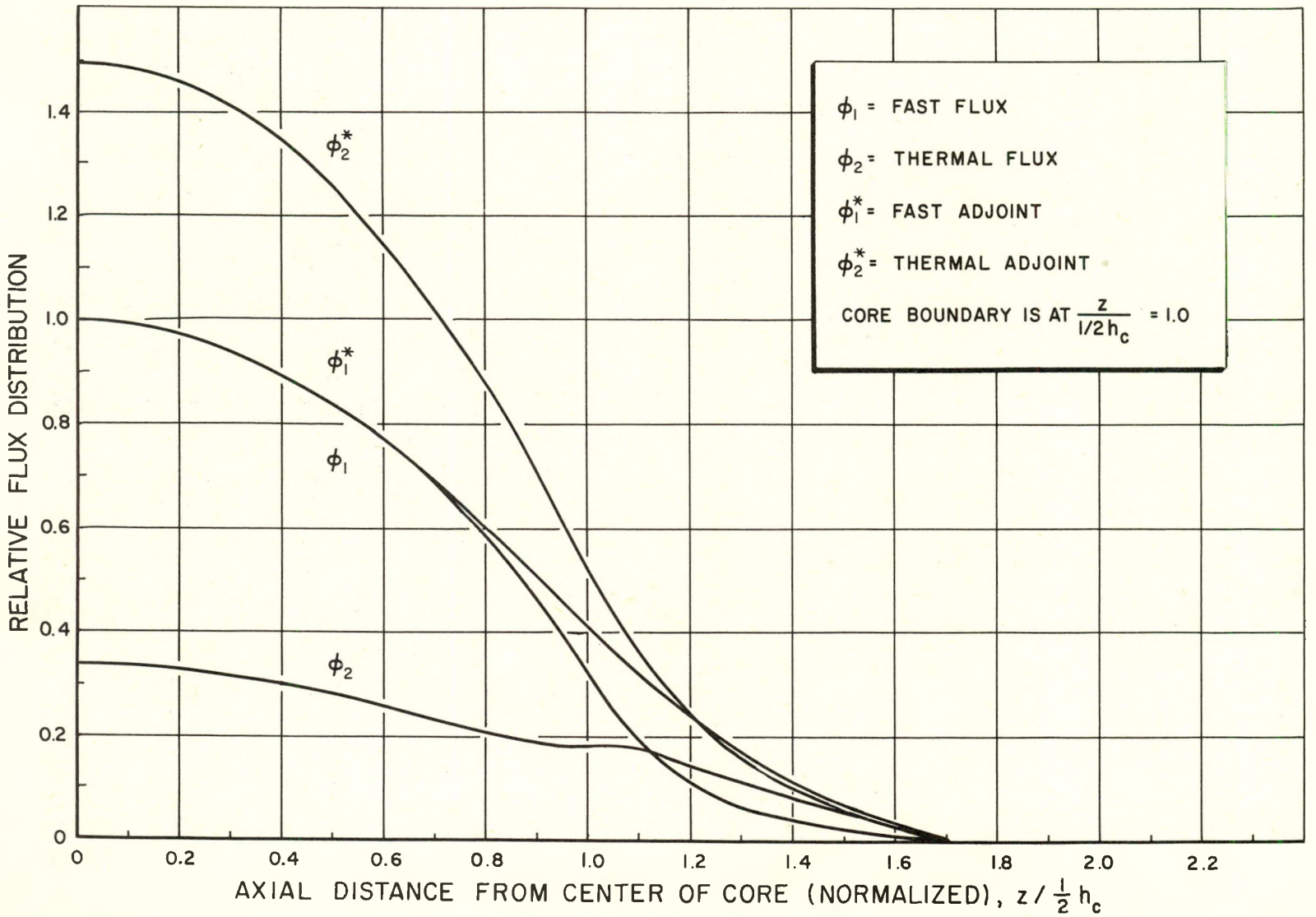

Fig. 5. Axial Flux Plot for the Dry Case

34

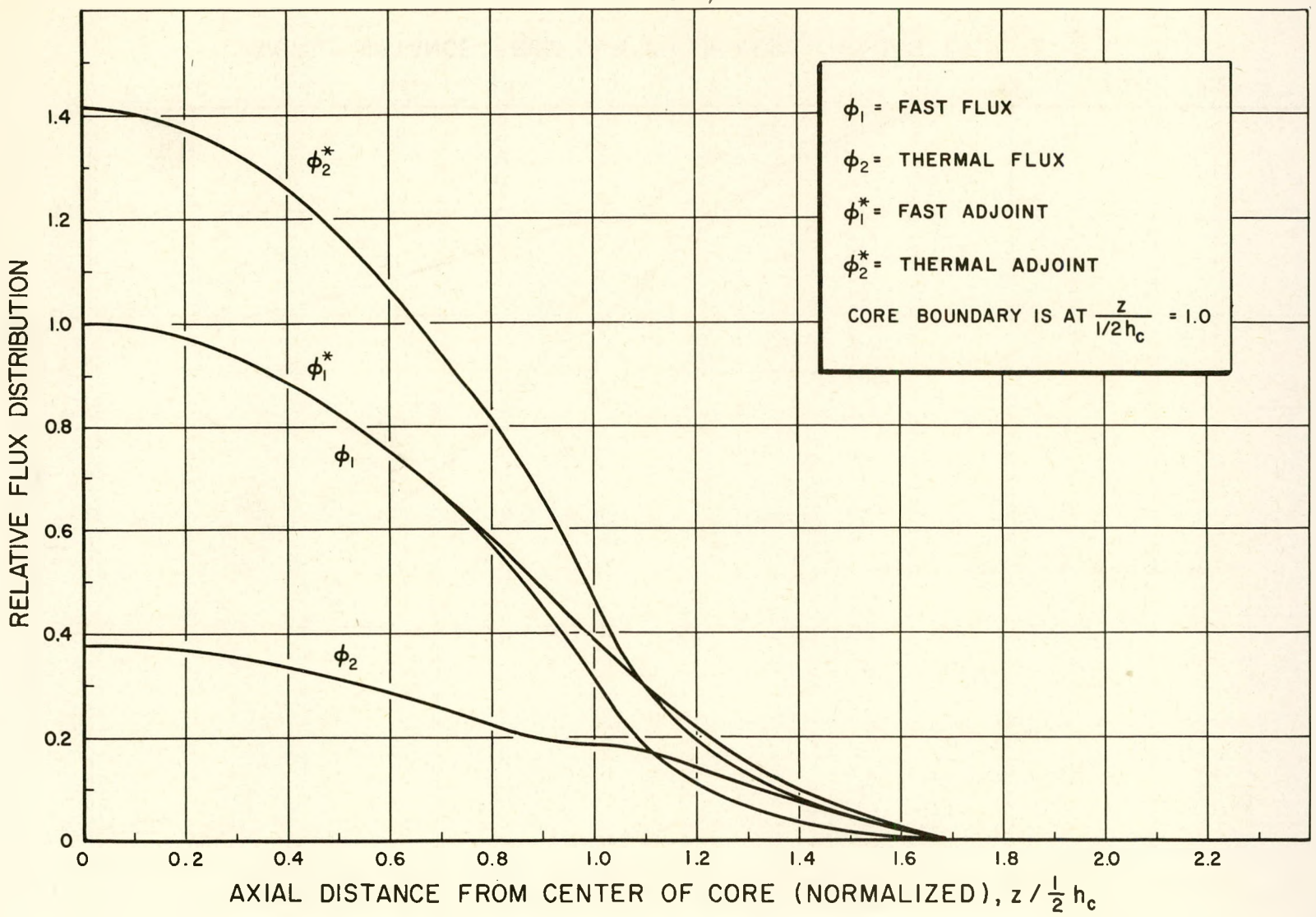

9693-52238

Fig. 6. Axial Flux Plot for the Wet Case

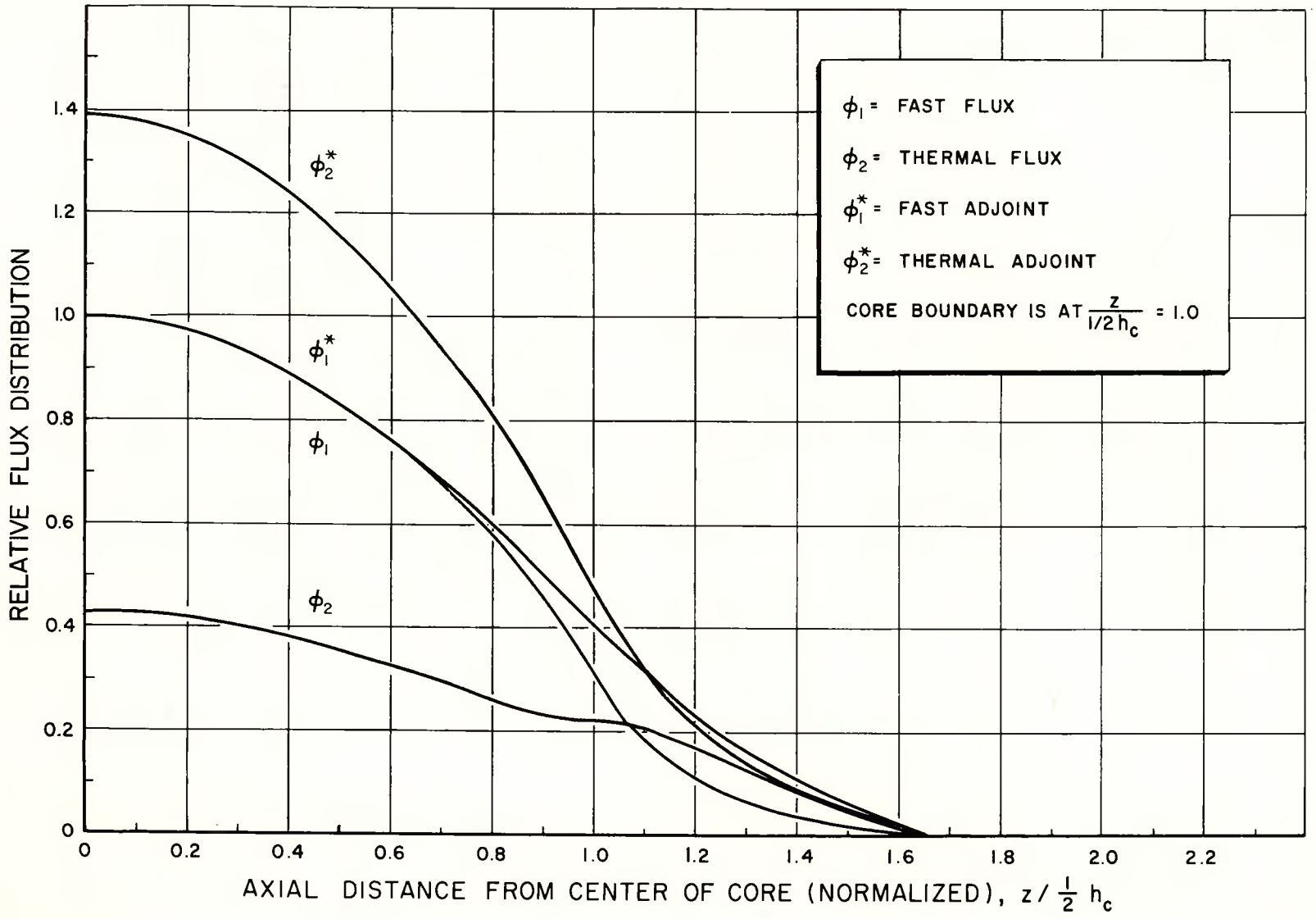

9693-52239

Fig. 7. Axial Flux Plot for the Hot Case

36

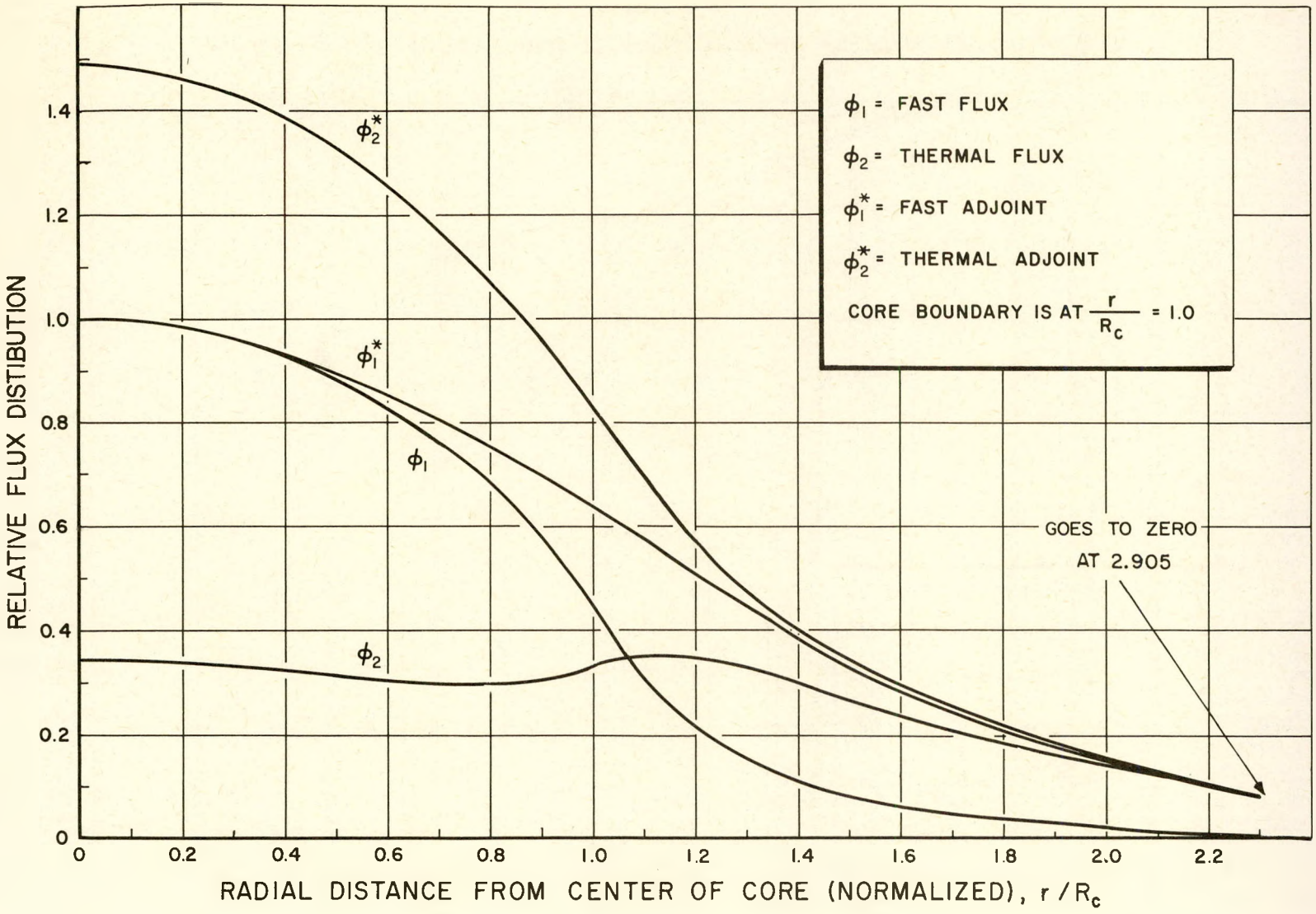

9693-52240

Fig. 8. Radial Flux Plot for the Dry Case

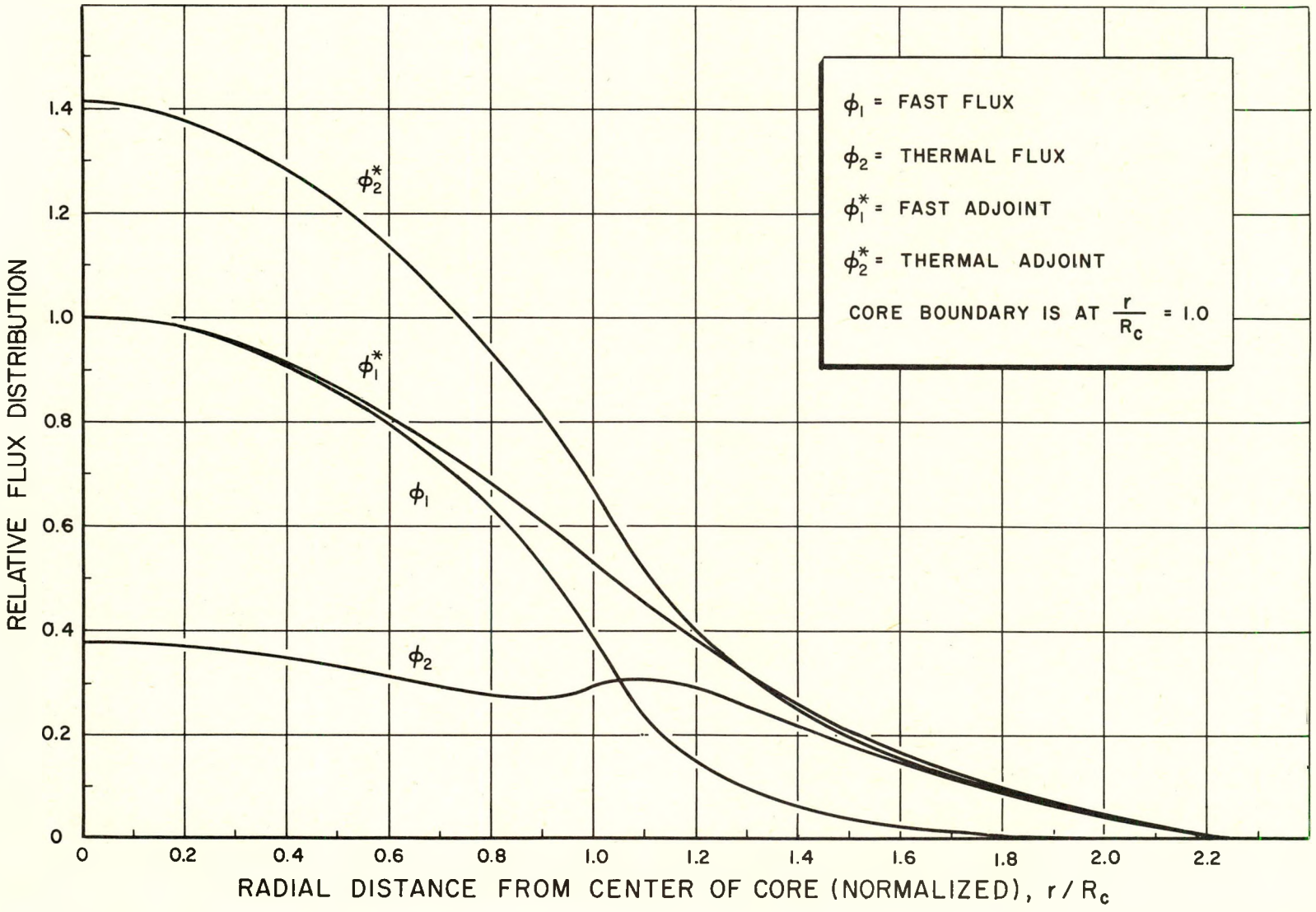

9693-52241

Fig. 9. Radial Flux Plot for the Wet Case

38

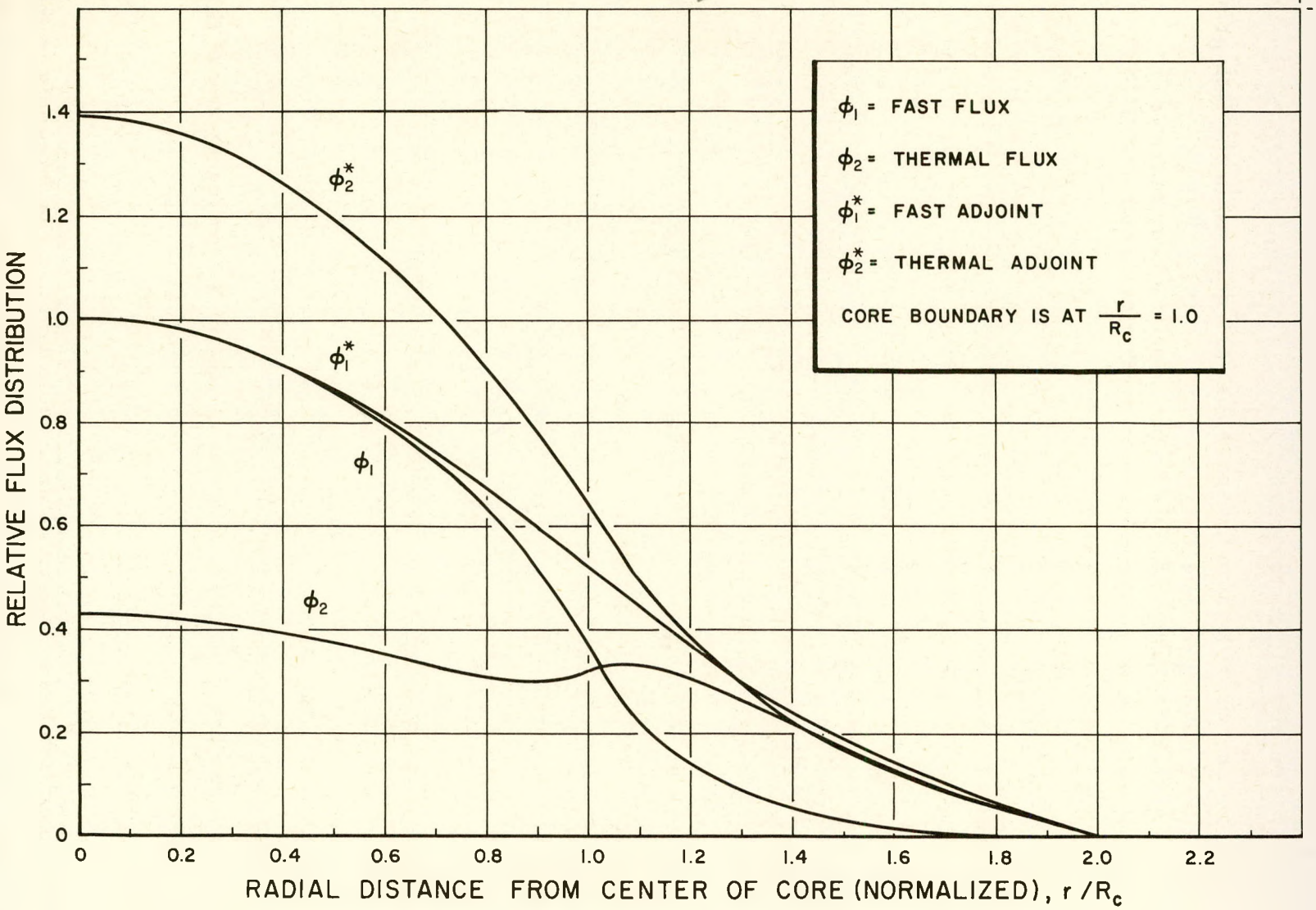

9693-52242

Fig. 10. Radial Flux Plot for the Hot Case

where

ω = reciprocal reactor period

β_i = fraction of fission neutrons that are delayed in the i-th group

λ_i = decay constant of the i-th group of delayed neutrons

ℓ = prompt generation time

ρ = reactivity

Using two group perturbation theory, one finds [9] that

$$\rho_i = \frac{\int \left[\begin{array}{l} -\phi_1^* \delta\Sigma_1 \phi_1' + \phi_1^* \delta(\frac{k}{p}\Sigma_2)\phi_2' + \phi_2^* \delta(p\Sigma_1)\phi_1' \\ -\phi_2^* \delta\Sigma_2 \phi_2' - \nabla\phi_1^* \cdot \delta D_1 \nabla\phi_1' - \nabla\phi_2^* \cdot \delta D_2 \nabla\phi_2' \end{array} \right] dV}{\int_{\text{core}} \phi_1^* \frac{k}{p}\Sigma_2 \phi_2' \, dV}$$

$$\ell = \frac{\int \left[\frac{\phi_1^* \phi_1'}{v_1} + \frac{\phi_2^* \phi_2'}{v_2} \right] dV}{\int_{\text{core}} \phi_1^* \frac{k}{p}\Sigma_2 \phi_2' \, dV}$$

where

ϕ^* = adjoint flux

ϕ' = perturbed flux

δq = the perturbation in the quantity q, where q represents any of the quantities Σ_i, k, etc.

v_i = velocity of neutrons in the i-th group.

Other quantities have definitions previously given. The integrals in the numerators are over the entire system--core and reflector. For the neutron velocities we take

$$v_1 = \frac{1}{\Sigma_1 \ell_1} = \frac{\ln E_1/E_2}{\sqrt{2m}\left(1/\sqrt{E}_2 - 1/\sqrt{E}_1\right)}$$

where

ℓ_1 = slowing down time in moderator

E_1 and E_2 = fission and thermal neutron energies, respectively.

$$v_2 = \sqrt{\frac{8kT}{\pi m}}$$

m = mass of the neutron

k = the Boltzman constant

T = average moderator temperature

The flux integrals were evaluated graphically for the hot case and the prompt generation time was found to be

$$\ell = 0.50 \times 10^{-3} \text{ seconds}$$

We now turn our attention to the reactivity. It is desired to find the change in the core size which is necessary to compensate for a given perturbation and leave the perturbed reactor in a steady state. This is done by evaluating ρ vs core radius and ρ for each perturbation. Knowledge of the total ρ of all the perturbations then enables us to determine the required change in core radius.

The perturbations evaluated were enrichment, fuel density, and stainless-steel cans at the edge of the reflector, the dummy fuel elements which occupy the unloaded process tubes in reflector cells that are adjacent to the core, and an increase of three in the number of stainless steel thimbles in the core. The quantities Σ_1, Σ_2, D_1, D_2, k, and p were evaluated for each of the above perturbations, using the recipes given in Sections IV and VI. Then we have

$$\delta q = q(\text{perturbed}) - q(\text{unperturbed})$$

A description of each perturbation follows. The actual SRE fuel is of enrichment = 0.02893 (instead of 0.02829) and density 19.03 gm/cm^3 (instead of 18.87). The moderator cells at the outer edge of the reflector are canned in stainless steel instead of zirconium. Several of these are incomplete cells, but the total is equivalent to 24 complete cells. The quantities q were averaged over a typical stainless steel-clad cell and the perturbed region is taken to be a ring at the outer edge of the reflector whose cross sectional area equals that of 24 cells. The dummy fuel elements consist of graphite cylinders which are canned in zirconium cans having a 2.5-inch OD and a 0.035-inch wall thickness. There are 12 additional process tubes provided in the reflector cells which are adjacent to the core and each of those tubes contain a dummy fuel element. The quantities q were averaged over a cell containing the dummy element, and the perturbed region was taken to be a ring around the unperturbed core whose cross-sectional area equals that of 12 cells. The perturbing effect of an additional stainless-steel thimble was obtained by adding a volume of stainless steel to the core equal to that contained in one thimble. The perturbation in q is just q(stainless steel) since it is assumed that core material is not displaced when the thimble is introduced. The perturbed region is the volume of the stainless steel, and as a typical example this was assumed to be located 40 centimeters from the axis of the core.

The reactivity due to a change of core radius was obtained by taking the perturbation to be a ring of core material around the unperturbed core whose cross-sectional area equals that of one cell. The perturbation was in all cases assumed to be constant over the perturbed region and zero elsewhere. The flux integrals for the hot case were evaluated by graphical integration over each of the perturbed regions. The reactivity due to each perturbation was calculated in units of ρ/β, which is customarily referred to as dollars. The results are given in Table X.

TABLE X

REACTIVITY DUE TO PERTURBATIONS

Perturbation Added	Reactivity (dollars)
1. One additional core cell	+ 0.54
2. Enrichment increase	+ 0.97
3. Fuel density increase	+ 0.10
4. Stainless steel reflector cans	- 0.04
5. 12 dummy fuel elements	- 0.35
6. 3 stainless steel thimbles	- 1.08
Net reactivity of 2, 3, 4, 5, and 6	- 0.40

It is therefore necessary to add 40/54 or 0.74 of a core cell to compensate for the perturbations 2, 3, 4, 5, and 6. This gives for the final critical loading in the hot-poisoned case 28.77 cells. This, of course, assumes no control rods in the reactor.

REFERENCES

1. R. C. Gerber, "Design of the Sodium Reactor Experiment," NAA-SR-Memo-1108, September 27, 1954.
2. The Brookhaven Neutron Cross Section Compilation Group, BNL-250 (1954).
3. The AEC Neutron Cross Section Advisory Group, AECD-2040 (5-15-52).
4. E. R. Cohen, "Standard Cross Sections and Reactor Physics Recipes," NAA-SR-Memo-1231 (1955).
5. F. L. Fillmore, "Some Observations Regarding the Resonance Escape Probability in Uranium-Graphite Lattices," NAA-SR-Memo-987 (1954).
6. G. W. Rodeback, "Temperatures Coefficient of Uranium and Thorium Resonance Integrals," NAA-SR-Memo-1301 (1955).
7. J. E. Garvey, "First Collision Probability in Hollow Cylinders," NAA-SR-Memo-1105 (1954).
8. E. R. Cohen, "Some Comments on the Effect of Epithermal Neutrons in a Reactor," NAA-SR-1127 (1955).
9. H. L. Garabedian, "Theory of Homogeneous Control of a Cylindrical Reactor," WAPD-19 (1950).